# Room-temperature ferromagnetism with high magnetic moment in Cu-doped AlN single crystal whiskers*

Jiang Liang-Bao(姜良宝), Liu Yu(刘 宇), Zuo Si-Bin(左思斌), and Wang Wen-Jun(王文军)†

*Research & Development Center for Functional Crystals, Beijing National Laboratory for Condensed Matter Physics, Institute of Physics, Chinese Academy of Sciences, Beijing* 100190, *China*

(Received 20 June 2014; revised manuscript received 20 October 2014; published online 10 December 2014)

Ferromagnetism is investigated in high-quality Cu-doped AlN single crystal whiskers. The whiskers exhibit room-temperature ferromagnetism with a magnetic moment close to the results from first-principles calculations. High crystallinity and low Cu concentrations are found to be indispensable for high magnetic moments. The difference between the experimental and theoretical moment values is explored in terms of the influence of nitrogen vacancies. The calculated results demonstrate that nitrogen vacancies can reduce the magnetic moments of Cu atom.

**Keywords:** spintronics, defects, nitrides, first-principles calculations

**PACS:** 75.50.–y, 71.55.–i, 61.72.uj, 71.15.Mb **DOI:** 10.1088/1674-1056/24/2/027503

## 1. Introduction

Over the past decade, many efforts have been devoted to AlN-based diluted magnetic semiconductors (DMSs).[1–6] Curie temperature ($T_c$) over 900 K was reported in Cr-doped AlN,[2] which was indeed an encouraging advance in the DMS research area. However, limited solubilities of transition metals in wide band gap (WBG) semiconductors often lead to the precipitation of clusters or second phases and complicate the investigations of magnetic properties in WBG semiconductors. In this regard, Cu doping is an ideal approach to solving this problem since neither Cu nor Cu-related precipitate contributes to ferromagnetism (FM). In fact, room-temperature ferromagnetism (RTFM) has been revealed in Cu-doped ZnO.[7–9] However, such observations have been attributed to defects.[8–10] RTFM has also been studied in Cu-doped AlN nanorods,[4] films,[11] and powders.[12] It was further investigated by x-ray absorption spectroscopy[13] and electron spin resonance.[14] However, there exist inconsistencies between theoretical predictions and experimental observations: Cu-doped AlN is predicted to yield an FM ground state with a magnetic moment of 2.0 $\mu_B$/Cu,[15,16] while the observed magnetic moments per Cu atom, however, are much smaller than the theoretical results. The large quantity of defects in these polycrystalline structures or nanostructures complicates the observed magnetism and makes the FM in Cu-doped AlN hard to understand.[12]

In this work, we synthesize a series of high-quality Cu-doped AlN single crystal whiskers exhibiting RTFM with relatively low Cu concentrations. The FM with the magnetic moment 1.6 $\mu_B$/Cu at room temperature (RT) is found to be consistent with our calculations, implying that the high magnetic moments are due to the high crystallinity and low Cu concentrations. To clarify the difference between the experimental results and the theoretical predictions, we study the magnetic moments of Cu atom under conditions with or without N vacancies ($V_N$s) in Cu-doped AlN by first-principles calculations. The results indicate that $V_N$s can suppress p–d hybridization between Cu-3d and N-2p states but does not affect its half-metallic behavior, thereby explaining that the observed moment is 25% lower than the calculated one.

## 2. Experimental procedure

The Cu-doped AlN whiskers were synthesized by reacting Al–Cu vapor with high-purity $N_2$ gas (99.999%) at high temperatures in an induction heating furnace, which is a modified physical vapor transportation process similar to that employed in Ref. [17]. The doping concentration of Cu was controlled by the mole ratio of Al and Cu in the raw material. In a typical procedure, Al powders (99.99%) and Cu powders (99.99%) with a mole ratio of 2:1 or 1:1 were mixed homogeneously and pressed into an Al–Cu ingot, which were denoted as S1 or S2, respectively. The ingots were loaded into a graphite crucible lined by a TaC layer to avoid contamination and then the crucible was placed into a graphite heater. After the induction heating furnace was evacuated to $1.0 \times 10^{-3}$ Pa, 0.6-atm (1 atm = $1.01325 \times 10^5$ Pa) $N_2$ as a nitrogen source was introduced into the furnace. During growth, the crucible was heated to 1400 K and kept at this temperature for 3 hours. Finally, it cooled down to room temperature (RT) naturally and the whiskers were collected from the surface of the TaC cover

*Project supported by the National Basic Research Program of China (Grant No. 2013CB932901), the National Natural Science Foundation of China (Grant Nos. 51372267, 51210105026, and 51172270), the Funds from the Chinese Academy of Sciences, the International Centre for Diffraction Data, USA (2013 Ludo Frevel Crystallography Scholarship Award), and the Funds from the Ministry of Education of China (2012 Academic Scholarship Award for Doctoral Candidates).

†Corresponding author. E-mail: wjwang@aphy.iphy.ac.cn

© 2015 Chinese Physical Society and IOP Publishing Ltd 

and analyzed. The nominal undoped AlN whiskers that underwent the same process (for more details of this sample, please refer to Ref. [17]) were served as references.

## 3. Results and discussion

The Cu concentrations in AlN are determined to be 0.05 at.% (S1) and 0.11 at.% (S2) by inductively coupled plasma-atomic emission spectrometry. The total concentration of magnetic impurities such as Fe, Mn is under a level of $10^{16}$ cm$^{-3}$ obtained by secondary ion mass spectrometry. Figure 1(a) shows the powder x-ray diffraction (PXRD) patterns of Cu-doped and undoped-AlN whiskers. All the PXRD patterns can be well indexed to a hexagonal wurtzite AlN cell (ICDD-PDF: 00-025-1133, space group $P63mc$, cell parameters $a = 3.1114$ Å and $c = 4.9792$ Å), indicating that no contribution from impurities or secondary phases induced by Cu doping is detected within the sensitivity of PXRD. Peak shape is sharp and clear, suggesting a high crystalline quality of whiskers. The evolutions of $a$ and $c$ with Cu concentration are shown in Fig. 1(b). The $a$ and $c$ of S2 are increased slightly by 0.002 Å and 0.006 Å, respectively, with the augment of Cu concentration, suggesting the incorporation of Cu atoms into the AlN lattice. Figure 2(a) shows a typical scanning electron microscope (SEM) image of S1. It can be seen that the whiskers are roughly uniform with diameters ranging from 1 μm to 3 μm. The enlarged SEM image of a single whisker from S1 in the inset of Fig. 2(a) indicates that the whiskers are smooth and straight. A typical high-resolution transmission electron microscope (HRTEM) image and a selected area electron diffraction (SAED) pattern (inset) of a single whisker from S1 are shown in Fig. 2(b). A fringe spacing of 0.501 nm between two adjacent planes in the HRTEM image is reasonably consistent with that of AlN (the ICDD data mentioned above), indicating that [0001] is the growth direction. The HRTEM and SAED images together establish the high monocrystalline nature of Cu-doped AlN whiskers. The RT micro-Raman spectra of Cu-doped and undoped-AlN whiskers in Fig. 2(c) show that all the Raman peaks correspond to the previously reported A1 (TO), $E_2$ (high), $E_1$ (TO), and $E_1$ (LO) modes, respectively.[18] The phonon modes of Cu-doped AlN undergo red shift compared with undoped AlN, which is attributed to the distortion of AlN crystals resulting from the Cu doping.[4] This further provides the evidence that Al atoms have been substituted by Cu atoms, which is consistent with the result of PXRD.

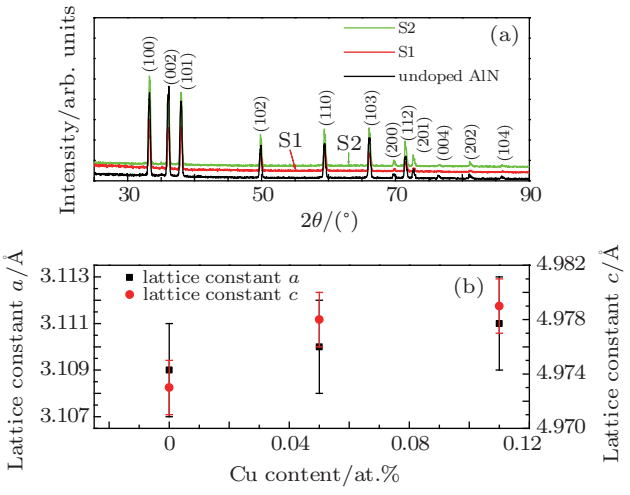



**Fig. 1.** (color online) (a) PXRD patterns of S1, S2, and undoped AlN whiskers. (b) The evolutions of cell parameters $a$ and $c$ of Cu-doped AlN whiskers with Cu concentration.

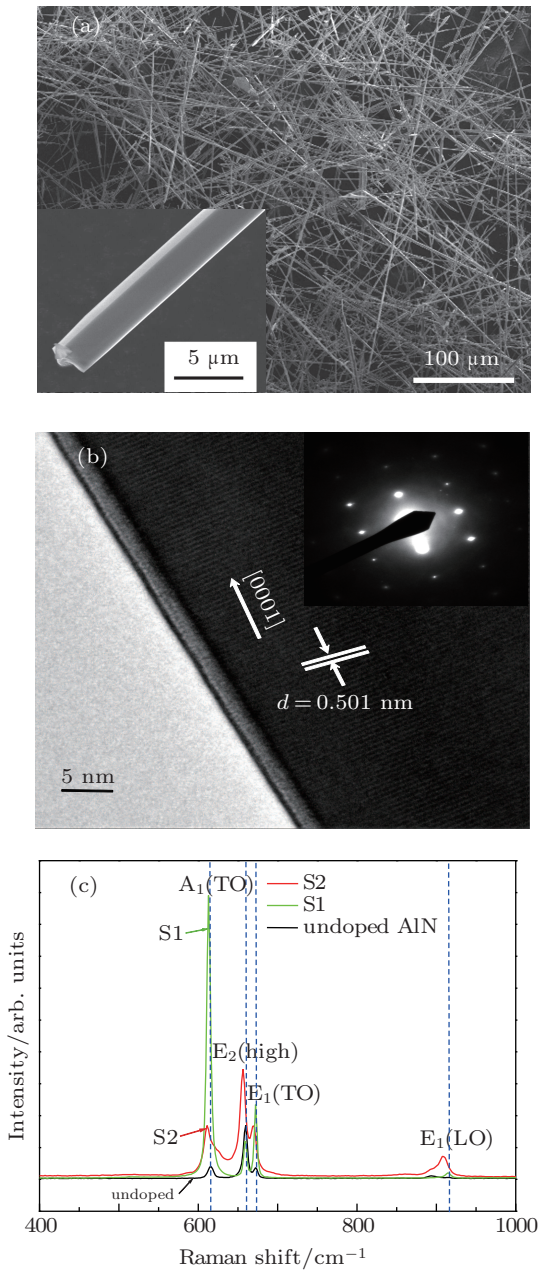



**Fig. 2.** (color online) (a) Typical SEM image of S1. Inset: the high-magnification SEM image of a single Cu-doped AlN whisker of S1. (b) The HRTEM image of S1. Inset: the SAED pattern of S1. (c) Raman spectra of S1, S2, and undoped AlN whiskers.

The magnetization measurements are performed on a superconducting quantum interference device vibrating sample

magnetometer which features a sensitivity of $10^{-7}$ emu. The diamagnetic behavior of nominal undoped AlN whiskers at 150 K rules out FM contamination in AlN whiskers [the inset of Fig. 3(a)]. The mass values of samples for magnetic measurements are 0.015 g of S1 and 0.01 g of S2 respectively. Figure 3(a) shows magnetic moment values each as a function of the magnetic field ($M$–$H$) of S1 and S2 at 150 K and 300 K. Both samples exhibit clear hysteresis loops, confirming RTFM ordering of Cu-doped AlN whiskers. The saturation magnetic moment values increase from 1.2 $\mu_B$/Cu to 1.9 $\mu_B$/Cu at 150 K and from 0.8 $\mu_B$/Cu to 1.6 $\mu_B$/Cu at RT with Cu concentration increasing from 0.05 at.% to 0.11 at.% without taking account of the weak paramagnetism or diamagnetism contribution. The magnetic moment per Cu atom at RT is much larger than that in earlier reports for Cu-doped AlN[4,11,12,14] and consistent with the calculations.[15,16] Compared with the previous results, the high monocrystalline nature is found to be indispensable for a large magnetic moment value. Besides, the relatively low Cu concentrations (much lower than those in Refs. [4] and [11]) and the separating impurity function in the AlN single crystal growth process eliminate the possibility of Cu clustering, leading to intrinsic magnetic moment values. Figure 3(b) shows the temperature dependences of the zero field cooled (ZFC) and field cooled (FC) magnetic moment value ($M$–$T$) at 500 Oe (1 Oe = 79.5775 A·m$^{-1}$). The smooth $M$–$T$ curves confirm the absence of additional magnetic phases.[19] The magnetizations remain up to 300 K, suggesting $T_c$ is above RT.

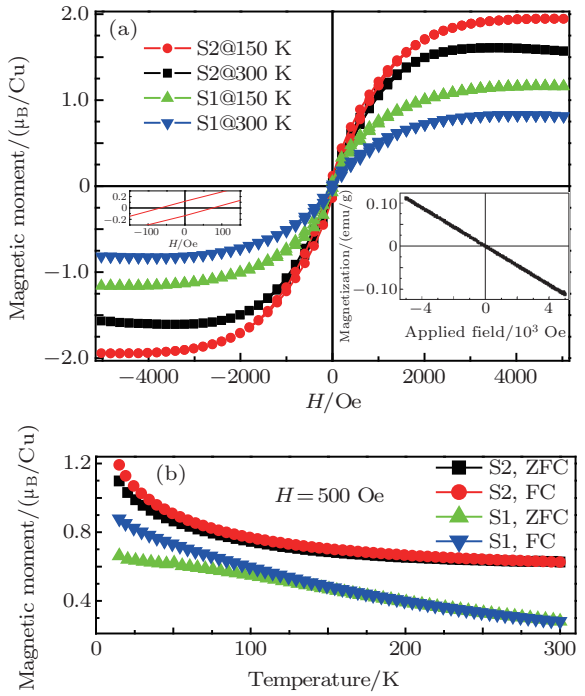



**Fig. 3.** (color online) (a) $M$–$H$ curves by cycling the field from 5 kOe to −5 kOe, and back to 5 kOe for S1 and S2 measured at 150 K and 300 K. Inset: the detail of the coercive field of S2 and the magnetization (in units of 1 emu/g = $10^{-3}$ Am$^2$/g) versus the magnetic field curve of undoped AlN at 150 K. (b) $M$–$T$ curves of S1 and S2.

To clarify the purity of the Cu powder used in our experiments, we measure the magnetization of the Cu powder alone. The mass of the measured Cu powder is 27.4 mg. Figure 4 shows the measured $M$–$H$ curves [(a) and (b)] and $M$–$T$ curves [(c)]. From the measurement results, we can see that the Cu powder shows paramagnetic behavior. Therefore, the magnetic impurities can be ruled out in the Cu-doped AlN samples in this work.

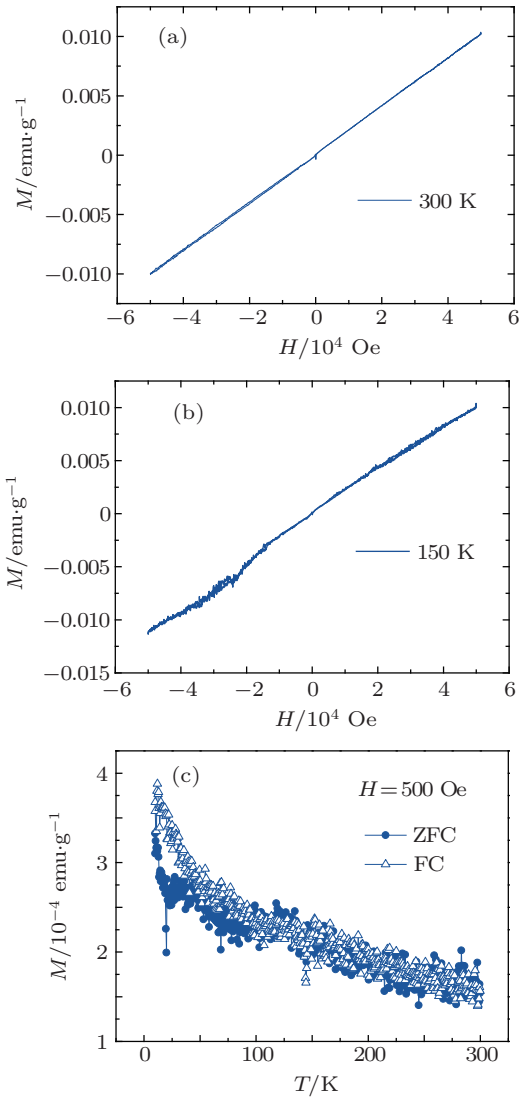



**Fig. 4.** (color online) (a) and (b) $M$–$H$ curves by cycling the field from 5 kOe to −5 kOe, and back to 5 kOe for Cu powder, measured at 150 K and 300 K. (c) $M$–$T$ curves of Cu powder.

Although the saturation magnetic moment value is raised a lot in our Cu-doped AlN samples, there is still a small discrepancy between the experimental and the predicted ones.[15,16] To understand this difference and get an insight into obtaining robust FM in Cu-doped AlN, first-principles calculations are performed in the Cambridge Serial Total Energy Package based on the spin-polarized density functional theory.[20] In our calculations, the generalized gradient approximation in the form of the Perdew–Burke–Ernzerhof func-

tion is used.[21] Self-consistent field calculations with a tolerance of $1.0 \times 10^{-6}$ eV/atom are performed with the cutoff energy set to be 320 eV using ultrasoft pseudopotentials.[22] The Monkhorst–Pack special $k$-point scheme with a grid spacing of 0.04 Å$^{-1}$ is used for the integration over the first Brillouin zone.[23]

The cell parameters $a$ and $c$ in 2H-AlN are respectively 3.127 Å and 5.013 Å after full geometry optimization for comparison, which have a tolerable error of 0.7% compared with the ICDD data of AlN mentioned above. As the case of one Al atom being replaced by Cu is more energy-favored than that of one N atom by Cu in AlN according to our calculations, Cu atoms are assumed only to take the Al positions. The 72-atom 3×3×2 AlN supercell with one Al atom substituted by a Cu atom is built for low Cu concentrations in our samples, which is a large supercell in contrast to that used in other studies.[15,16,24,25] After fully relaxed calculation, the corresponding $a$ and $c$ are slightly changed by 0.002 Å and 0.003 Å, respectively. The spin-polarization energy (the energy difference between the spin-polarized and spin-unpolarized states) of this supercell is 387 meV, suggesting that the spin-polarized state is stable well above RT.[17] In such a Cu concentration, doped AlN still possesses half-metallic [see Fig. 5(a)] and FM behaviors with a nearest-neighbor exchange interaction energy of 12.1 meV. The calculated magnetic moment is 2.0 $\mu_B$/Cu, consistent with those given by the earlier reports[15,16] but larger than the experimental result 1.9 $\mu_B$/Cu (S2) at 150 K.

As Cu-doped AlN whiskers have high crystallinity and no other impurities, $V_N$s should be taken into account because of their low formation energy in AlN.[26,27] After introducing one $V_N$ into the Cu-doped AlN supercell, the corresponding $a$ and $c$ changes of 0.003 Å and 0.006 Å are consistent with the PXRD results, indicating that the existence of $V_N$s is reasonable. It is found that the magnetic moment decreases to 1 $\mu_B$/Cu with the spin-polarization energy being 208 meV. Hence, when $V_N$ is introduced into the Cu-doped AlN lattice, the average magnetic moment will decrease, while its half-metallic behavior is found to maintain there from Fig. 5(b). Furthermore, the partial spin-resolved densities of states (DOSs) calculated for the Cu-doped AlN supercells without and with a $V_N$ presented in Figs. 5(a) and 5(b) indicate the existence of p–d hybridization between N-2p and Cu-3d states, which contributes significantly to the minority-spin states. Figures 5(c) and 5(d) show the charge densities of the total spin states around the Cu-dopant site without and with a $V_N$. The shape of the charge density in Fig. 5(c) shows clearly that the spin polarizations of N-2p and Cu-3d interact along each direction of Cu–N bonding around the Cu-dopant site. However, in Fig. 5(d), the spin density around three of four N atoms vanishes. The spin polarization is only along one Cu–N bonding direction, which can be attributed to the weakening of p–d hybridization due to $V_N$s. This reasonably explains that the magnetic moments in Cu-doped AlN decrease with $V_N$s.

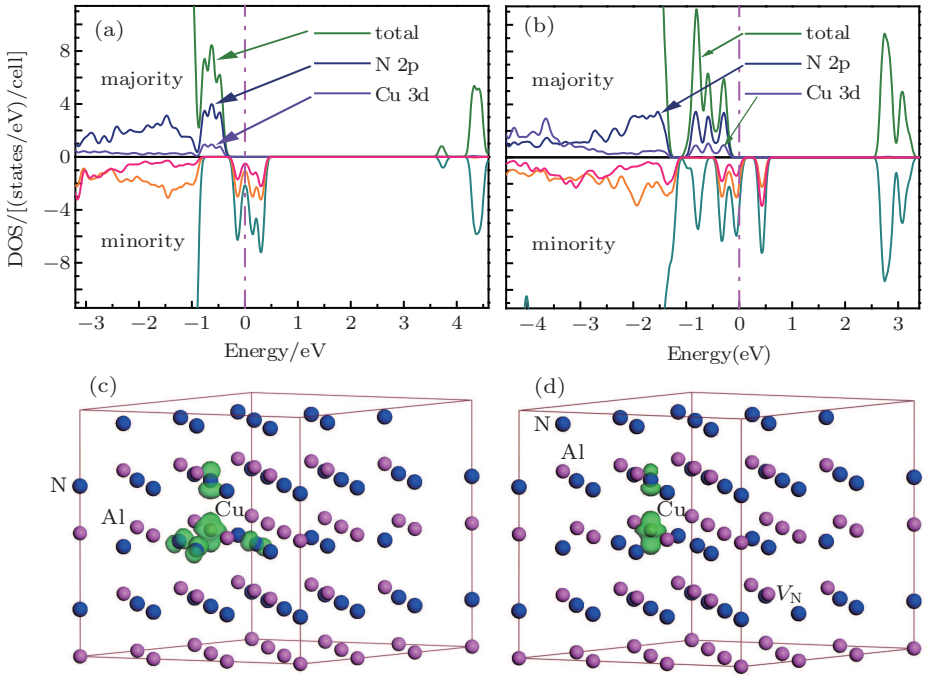



**Fig. 5.** (color online) (a) and (b) Total and partial (2p orbitals of four N atoms around a Cu atom and 3d orbitals of the Cu atom) spin-resolved DOSs in the Cu-doped AlN supercells without or with a $V_N$. (c) and (d) Total spin density isosurface (isovalue is 0.11 e/Å$^3$) around the Cu-dopant site without or with a $V_N$. Cu atoms are located inside the isosurface and an arrow indicates the location of the $V_N$.

According to the calculated results, the concentrations of $V_N$ involved in suppressing the FM of Cu doping are about 0.04 at.% and 0.01 at.% for S1 and S2, respectively. Such a difference may be due to the nonuniform $V_N$ distribution. The total $V_N$ concentrations should be the same because the samples are synthesized under the same condition. It is known that vacancies can also contribute to FM in WBG semiconductors,[17,28] which may also make these concentrations a little higher. Although $V_N$s can be manipulated conveniently,[3,17] it is difficult to reduce the $V_N$ concentration to a level low enough to completely remove their effect on magnetism. Luckily, the introduction of $V_N$s does not change the half-metallic behavior. So magnetic moments of Cu-doped AlN slightly lower than 2.0 $\mu_B$/Cu will be tolerable. Besides, $V_N$s may be beneficial to FM in Cu-doped AlN, as it is reported that vacancies play important roles in inducing FMs in Cr-doped AlN and Cu-doped ZnO.[27,29]

It is difficult to increase magnetic moment values in doped AlN. The magnetic moment of the most attractive Cr-doped AlN reaches only 0.7 $\mu_B$/Cr,[30] while the predicted value is 3.0 $\mu_B$/Cr.[31] We demonstrate that the FM with magnetic moment approaching the predicted value can be achieved without other magnetic component interference in Cu-doped AlN whiskers as long as they have high crystallinity and relatively low Cu concentrations. Our results do not only verify the RTFM of Cu-doped AlN, but also raise its feasibility of spintronic applications.

## 4. Conclusions

In this paper, RTFM is observed in high-quality Cu-doped AlN single crystal whiskers with Cu concentrations less than 0.11 at.%, which are synthesized by metal nitriding. The large magnetic moment at RT (1.6 $\mu_B$/Cu) is observed, which is close to the first-principles calculation result (2.0 $\mu_B$/Cu). The result implies that high crystallinity and relatively low Cu concentrations are indispensable for Cu-doped AlN to obtain high magnetic moments. We attempt to explain the difference between the measured and predicted results with considering the existence of $V_N$s. The Cu-doped AlN proves to maintain the half-metallic behavior, while its magnetic moment value decreases due to the suppression of p–d hybridization induced by $V_N$s. Our results provide a route to obtain Cu-doped AlN with RTFM and gain an insight into obtaining robust FM in it, which will be helpful for its potential applications in spintronics.

## Acknowledgment

Dr. Y. Liu would like to thank Dr. G. Wang, Dr. L. L. Chen and Dr. Z. L. Li of the Institute of Physics, Chinese Academy of Sciences for their fruitful discussion.

## References

[1] Frazier R, Thaler G, Overberg M, Gila B, Abernathy C R and Pearton S J 2003 *Appl. Phys. Lett.* **83** 1758
[2] Liu H X, Wu S Y, Singh R K, Gu L, Smith D J, Newman N, Dilley N R, Montes L and Simmonds M B 2004 *Appl. Phys. Lett.* **85** 4076
[3] Zhang J, Li X Z, Xu B and Sellmyer D J 2005 *Appl. Phys. Lett.* **86** 212504
[4] Ji X H, Lau S P, Yu S F, Yang H Y, Herng T S and Chen J S 2007 *Nanotechnology* **18** 105601
[5] Ji X H, Lau S P, Yu S F, Yang H Y, Herng T S, Sedhain A, Lin J Y, Jiang H X, Teng K S and Chen J S 2007 *Appl. Phys. Lett.* **90** 193118
[6] Li H, Bao H Q, Song B, Wang W J and Chen X L 2008 *Solid State Commun.* **148** 406
[7] Buchholz D B, Chang R P H, Song J H and Ketterson J B 2005 *Appl. Phys. Lett.* **87** 082504
[8] Xu Q Y, Schmidt H, Zhou S Q, Potzger K, Helm M, Hochmuth H, Lorenz M, Setzer A, Esquinazi P, Meinecke C and Grundmann M 2008 *Appl. Phys. Lett.* **92** 082508
[9] Li T J, Li G P, Gao X X and Chen J S 2010 *Chin. Phys. Lett.* **27** 087501
[10] Xu Q Y, Zheng X H and Gong Y P 2010 *Chin. Phys. B* **19** 077501
[11] Ran F Y, Subramanian M, Tanemura M, Hayashi Y and Hihara T 2009 *Appl. Phys. Lett.* **95** 112111
[12] Li H, Chen X L, Song B, Bao H Q and Wang W J 2011 *Solid State Commun.* **151** 499
[13] Guda A A, Lau S P, Soldatov M A, Smolentsev N Y, Mazalova V L, Ji X H and Soldatov A V 2009 *J. Phys.: Conf. Ser.* **190** 012136
[14] Ran F Y, Subramanian M, Tanemura M, Hayashi Y and Hihara T 2010 *Physica B* **405** 3952
[15] Wu Q Y, Huang Z G, Wu R and Chen L J 2007 *J. Phys.: Condens. Matter* **19** 056209
[16] Jia W, Han P, Chi M, Dang S H, Xu B S and Liu X G 2007 *J. Appl. Phys.* **101** 113918
[17] Liu Y, Jiang L B, Wang G, Zuo S B, Wang W J and Chen X L 2012 *Appl. Phys. Lett.* **100** 122401
[18] Jiang L B, Li H, Zuo S B, Bao H Q, Wang W J and Chen X L 2010 *Appl. Phys. A* **100** 545
[19] Song B, Bao H Q, Li H, Lei M, Jian J K, Han J C, Zhang X H, Meng S H, Wang W Y and Chen X L 2009 *Appl. Phys. Lett.* **94** 102508
[20] Clark S J, Segall M D, Pickard C J, Hasnip P J, Probert M J, Refson K and Payne M C 2005 *Z. Kristallogr.* **220** 567
[21] Perdew J P, Burke K and Ernzerhof M 1996 *Phys. Rev. Lett.* **77** 3865
[22] Vanderbilt D 1990 *Phys. Rev. B* **41** 7892
[23] Monkhorst H J and Pack J D 1976 *Phys. Rev. B* **13** 5188
[24] Kang B S, Lee J K, Lim Y S, Song K M and Chae K P 2011 *J. Magn.* **16** 332
[25] Kang B S, Lee J K, Chae K P, Kim K S, Zhang Y D, Yu S C and Oh S K 2012 *IEEE T. Magn.* **48** 1285
[26] Zhang Y, Liu W and Niu H B 2008 *Phys. Rev. B* **77** 035201
[27] Shi L J, Zhu L F, Zhao Y H and Liu B G 2008 *Phys. Rev. B* **78** 195206
[28] Liu Y, Wang G, Wang S C, Yang J H, Chen L, Qin X B, Song B, Wang B Y and Chen X L 2011 *Phys. Rev. Lett.* **106** 087205
[29] Herng T S, Qi D C, Berlijn T, Yi J B, Yang K S, Dai Y, Feng Y P, Santoso I, Sánchez-Hanke C, Gao X Y, Wee A T S, Ku W, Ding J and Rusydi A 2010 *Phys. Rev. Lett.* **105** 207201
[30] Kumar D, Antifakos J, Blamire M G and Barber Z H 2004 *Appl. Phys. Lett.* **84** 5004
[31] Cui X Y, Delley B, Freeman A J and Stampfl C 2006 *Phys. Rev. Lett.* **97** 016402